# University of Siegen

## Manual

## Surface plasmon resonance (SPR) based sensing

**Prepared by**

Assegid M. Flatae
Philipp Reuschel
Mario Agio

## Contents


Learning objectives ……. 03

1. Introduction and theoretical background……. 03

    1.1 Optics in metals……... 04

    1.2 Bulk plasmons……. 05

    1.3 Surface plasmon polariton……... 07

2. Experimental background……... 10

    2.1 Coupling light to surface plasmon polaritons and sensing….. 10

    2.2 Experimental setup for detecting SPR…… 11

3. Procedures ……. 13

    3.1 Excitation of surface plasmon polaritons…….. 13

    3.2 Sensing of fluid……. 13

    3.3 Data analysis and report format…… 13

4. References……. 14

**Learning objectives:**

- In this laboratory experiment, students will become familiar with the fundamental concepts of surface plasmon resonance (SPR) and apply these principles to demonstrate the sensitivity of SPR to surface-related phenomena in sensing applications.
- The experimental results will be compared with theoretical values of the physical quantities associated with the detected materials to determine the experimental error and evaluate the sensitivity of the SPR sensor.

## 1. Introduction and Theoretical background

Long before scientists began exploring the optical properties of metal nanostructures and surface plasmons, artists were already harnessing these effects to create vivid colours in glass artifacts and artworks. By incorporating gold nanoparticles of varying sizes into glass, they produced a remarkable spectrum of colors. A famous example is the Lycurgus Cup from the Roman Empire (4th century AD), which appears green under reflected light but glows red when light passes through it. Similar techniques were also used in stained glass windows found in churches.

Figure 1. The Lycurgus cup (1958,1202.1) in reflected (left) and transmitted (right) light. Department of Prehistory and Europe, The British Museum.

The study of electromagnetic phenomena at metal–dielectric interfaces has seen a significant interest in recent years, a trend that traces back to the pioneering work of Gustav Mie (1908) [1] and others on small metal particles and flat surfaces. This growing attention is further driven by advances in nanofabrication techniques, such as electron beam lithography and ion beam milling, as well as by modern characterization methods like near-field microscopy.

A surface plasmon polariton (SPP) is a coherent oscillation of free electrons that occurs at the interface between a metal and a dielectric. These excitations manifest as electromagnetic waves confined to the surface, arising from their strong coupling with the conductor's free electrons—hence the term *polaritons*, which emphasizes their hybrid light-matter nature. In this interaction, the free electrons collectively oscillate in resonance with the incident electromagnetic wave, enabling the localization and guiding of light at subwavelength scales. The first observation of surface plasmon polaritons (SPPs) was reported by A. Otto in 1968 [2], with a significant improvement to the experimental setup introduced by E. Kretschmann in 1971 [3]. Over the past few decades, the properties of SPPs and their wide-ranging applications have been extensively

investigated, leading to the emergence of a dedicated research field known as *plasmonics*. Modern applications of plasmonics encompass a wide range of technologies, including the use of metal nanostructures as nanoantennas for optical sensing in biological and chemical systems, as well as the development of subwavelength waveguides. These structures enable the concentration and manipulation of light at scales below the diffraction limit, paving the way for highly compact photonic circuits with dimensions far smaller than those achievable with conventional optics [4,5]. One of the most compelling features of surface plasmon polaritons (SPPs) is their ability to enhance the surface sensitivity of various spectroscopic techniques, including Raman scattering, fluorescence, and harmonic generation. In their simplest implementation, reflectivity-based measurements can serve as highly sensitive biosensors for chemical detection, monitoring molecular adsorption—such as polymers, DNA, or proteins—and investigating interactions between a wide range of biomolecules, including nucleic acids, receptors, peptides, proteins, antibodies, and lipids. Furthermore, SPP-based biosensors have proven valuable for studying viral binding to functionalized surfaces and hold promise as powerful tools in antiviral drug discovery. These capabilities have driven the development of commercial sensing platforms, such as Biacore systems, which have been followed by numerous other technologies.

In the following, the fundamental principles of SPPs and their excitation mechanisms relevant to sensing applications will be discussed.

### 1.1 Optics in metals

Metals are highly reflective for frequencies up to the visible spectrum, preventing electromagnetic waves from propagating through them. This property makes metals ideal for cladding layers in waveguides and resonators, especially at microwave and far-infrared frequencies. In the low-frequency regime, metals are often treated as perfect or good conductors with infinite or fixed finite conductivity, as only a negligible amount of electromagnetic waves penetrate the metal.

However, as the frequency increases toward the near-infrared and visible parts of the spectrum, field penetration into the metal increases, resulting in greater dissipation. This phenomenon limits the simple scaling of photonic devices from low to high frequencies. At ultraviolet frequencies, metals begin to exhibit dielectric behavior, allowing the propagation of electromagnetic waves with varying attenuation, which depends on the metal's electronic band structure.

For alkali metals like sodium, which exhibit a nearly free-electron response, ultraviolet transparency is observed. In contrast, noble metals such as gold and silver experience significant absorption in this range due to electronic band transitions. These dispersive properties are captured by the complex, frequency-dependent dielectric function, $\varepsilon(\omega)$, which determines the behavior of metals across different frequency regimes..

The interaction of metals with electromagnetic fields is well described within a classical framework of Maxwell’s equations [6]. Even metallic nanostructures with dimensions on the order of a few nanometres can often be accurately modeled without involving quantum mechanics. This is largely due to the high density of free electrons in metals, which leads to extremely narrow energy level spacings—much smaller than the thermal energy $k_B T$ at room temperature—thereby minimizing the influence of quantum effects in many cases.

In a simplified framework, the interaction of metals with electromagnetic fields using the classical Maxwell equations read:

$$\begin{aligned} \nabla \cdot \mathbf{D} &= \rho \\ \nabla \cdot \mathbf{B} &= 0 \\ \nabla \times \mathbf{E} &= -\partial \mathbf{B}/\partial t \\ \nabla \times \mathbf{H} &= \mathbf{J} + \partial \mathbf{D}/\partial t, \end{aligned}$$

The relation connects the macroscopic fields (dielectric displacement ***D***, electric field ***E***, magnetic field ***H*** and magnetic induction ***B***) with an external charge density ρ and current density ***J***.

In the case of linear, isotropic, and non-magnetic media, the constitutive relations are given by:

$$\begin{aligned} \mathbf{D} &= \epsilon_0 \epsilon \mathbf{E} \\ \mathbf{B} &= \mu_0 \mathbf{H} \end{aligned}$$

with a frequency dependent dielectric constant: ε = ε(ω), which is in general a complex function, $\varepsilon = \varepsilon' + i\varepsilon''$. It is furthermore connected to the complex index of refraction via $n + i\kappa = \sqrt{\varepsilon}$. Explicitly one can obtain the following expressions:

$$\begin{aligned} \epsilon' &= n^2 - \kappa^2, & \epsilon'' &= 2n\kappa, \\ n^2 &= \frac{\epsilon'}{2} + \frac{1}{2}\sqrt{\epsilon'^2 + \epsilon''^2}, & \kappa &= \frac{\epsilon''}{2n} \end{aligned}$$

The real part of the refractive index n(ω) is responsible for dispersion, the imaginary part κ(ω) (extinction coefficient) determines absorption. Beer's law describes the exponential decay of the intensity *I* of a light beam (along the *x*-direction) in a medium: $I(x) = I_0 \exp(-\alpha x)$, where $\alpha(\omega) = 2\kappa(\omega)\omega/c$ is the absorption coefficient.

### 1.2 Bulk plasmons

The optical properties of metals can be described over a large frequency range using the Drude model, where an electron gas (effective electron mass *m*) of density *N* is assumed to freely propagate in a background of positively charged ions. These electrons will oscillate in the presence of an electromagnetic field $\boldsymbol{E}(t) = \boldsymbol{E}_0 \exp(i\omega t)$ and are damped through collisions with a rate $\gamma = 1/\tau$ (typically $\tau = 10^{-14}$ s at room temperature). The equations of motion in the Drude model are thus:

$$m\ddot{\mathbf{x}} + m\gamma\dot{\mathbf{x}} = -e\mathbf{E}(\mathbf{t})$$

with the stationary solution

$$\mathbf{x}(\mathbf{t}) = \frac{e}{m(\omega^2 + i\gamma\omega)}\mathbf{E}(\mathbf{t})$$

The electrons, which are displaced by **x** relative to the fixed ions, generate a polarisation $\boldsymbol{P} = -Ne\boldsymbol{x}$. It follows for the dielectric displacement and the dielectric constant:

$$\begin{aligned}
\mathbf{D} &= \epsilon_0 \mathbf{E} + \mathbf{P} = \epsilon_0 \epsilon \mathbf{E} \\
&= \epsilon_0 \left(1 - \frac{\omega_p^2}{\omega^2 + i\gamma\omega}\right) \mathbf{E} \\
\Rightarrow \epsilon(\omega) &= 1 - \frac{\omega_p^2}{\omega^2 + i\gamma\omega} = 1 - \frac{\omega_p^2 \tau^2}{\omega^2 \tau^2 + i\omega\tau},
\end{aligned}$$

where we introduced the plasmon frequency $\omega_p^2 = Ne^2/(\varepsilon_0 m)$.

At low frequencies the absorption coefficient becomes $\alpha = \sqrt{2\omega_p^2 \omega\tau/c^2}$ and the penetration depth of the electromagnetic field, after Beer's law, becomes $\delta = 2/\alpha$ and it is called skin depth. However, at large frequencies, i.e. $\omega\,\tau >> 1$, the damping term $i\omega\tau$ can be neglected and $\varepsilon(\omega)$ becomes approximately real:

$$\epsilon(\omega) = 1 - \frac{\omega_p^2}{\omega^2}$$

The dispersion relation of electro-magnetic fields can be determined from $\kappa^2 = \varepsilon\omega^2/c^2$.

$$\omega(k) = \sqrt{\omega_p^2 + k^2/c^2}$$

As can be also seen in Figure 2, there is no propagation of electromagnetic waves below the plasmon frequency $\omega < \omega_p$. For $\omega > \omega_p$ waves propagate with a group velocity $v_g = d\omega/dk < c$. Of further interest is the special case $\omega = \omega_p$, where for low damping $\varepsilon(\omega_p) = 0$. One can show that here a collective longitudinal excitation mode (***k*** // ***E***) is formed (see Ref. [6]).

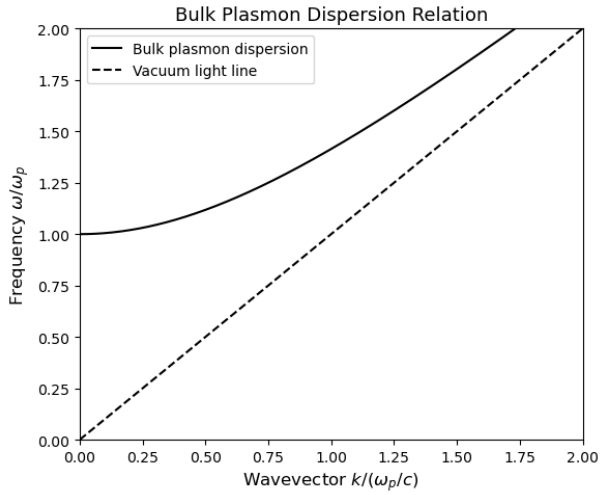


**Figure 2**. Dispersion relation of the free electron gas.

Physically, plasmons arise from the collective oscillation of the conduction electron gas relative to the fixed lattice of positive ions. The quanta associated with these charge density oscillations are referred to as *plasmons*—or more specifically, *bulk plasmons* to distinguish them from surface plasmons discussed in later sections. As longitudinal waves, bulk plasmons cannot directly couple to transverse electromagnetic fields, and therefore cannot be excited or detected through conventional far-field radiation. In most metals, the plasma frequency lies in the ultraviolet range, with corresponding energies typically between 5 and 15 eV, depending on the specific band structure of the material.

### 1.3 Surface plasmon polaritons (SPPs)

SPPs are electromagnetic excitations that propagate along the interface between a metal and a dielectric medium. To derive the conditions for their existence, we once again begin with Maxwell's equations, which must be solved separately for the metallic and dielectric regions. As a starting point, consider a flat metal surface extending infinitely in the *xy*-plane, with the interface located at $z = 0$ (see Fig. 3 and also Ref. 9).

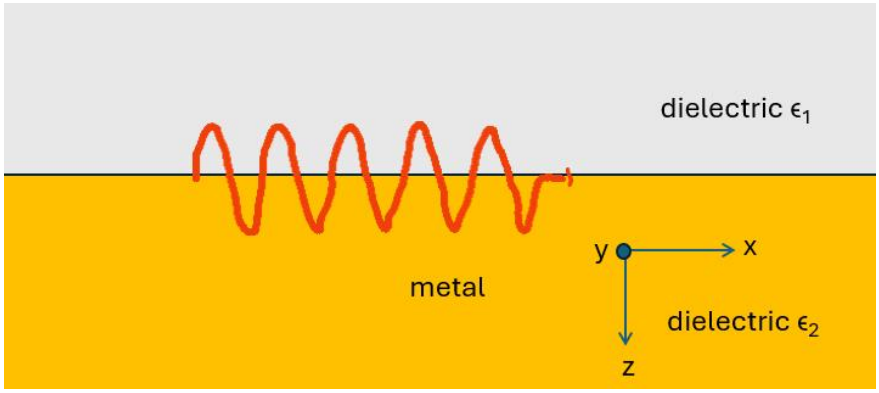


**Figure 3**. The interface along the *xy*-plane between a dielectric material (top) and a metallic surface (bottom).

The conditions for the continuity of the normal and transversal field components on this interface (see e.g. J.D. Jackson, "`Classical Electrodynamics"') are given by:

$$D_{1,z} = D_{2z}, \qquad B_{1,z} = B_{2,z}$$
$$E_{1,x/y} = E_{2x/y}, \qquad H_{1,x/y} = H_{2,x/y}$$

where the indices (1) and (2) indicate dielectric and metal, respectively. One can show (see Ref. 6) that under these conditions no transverse-electric (TE) modes can exist. Instead we directly start with an *ansatz* for a transverse-magnetic (TM) mode, which propagates along the x direction ($i$ = 1,2):

$$\begin{aligned} \mathbf{E}_i &= (E_{i,x}, 0, E_{i,y}) e^{i(\mathbf{k}_i \cdot \mathbf{r} - i\omega t)} \\ \mathbf{H}_i &= (0, H_{i,y}, 0) e^{i(\mathbf{k} \cdot \mathbf{r} - i\omega t)} \\ \mathbf{D}_i &= \epsilon_0 \epsilon_i \mathbf{E}_i, \qquad \mathbf{B}_i = \mu_0 \mathbf{H}_i \end{aligned}$$

The wave vector is given by $\boldsymbol{k}_i = (\beta, 0, k_{i,z})$, where $\beta = k_x$ indicates the propagation constant along *x*. Using this approach with the conditions of continuity from above and the Maxwell's equation in absence of charges and currents ($\rho = 0$, $\boldsymbol{J} = 0$), we obtain the following relations between the $k_{i,z}$ components:

$$\frac{k_{1,z}}{\epsilon_1} = \frac{k_{2,z}}{\epsilon_2}$$

We are looking for solutions that describe modes bound to the interface. Thus, the $k_{i,z}$ components have to be imaginary and of opposite sign:

$$k_{1,z} = +i\kappa_1$$

In this way, the fields decay exponentially into the respective half spaces: $\boldsymbol{E}_i \propto exp(\pm ik_{i,z}) = exp(\pm k_{i,z})$, as also symbolized in Fig. 4. Comparing the above two relations, one can directly see that this is fulfilled only, if the dielectric constants of the two materials are of opposite sign (i.e. $\varepsilon_1 = -\varepsilon_2$). Surface plasmons can thus indeed only exist at the interface between a metal ($\varepsilon < 0$) and a dielectric medium ($\varepsilon > 0$).

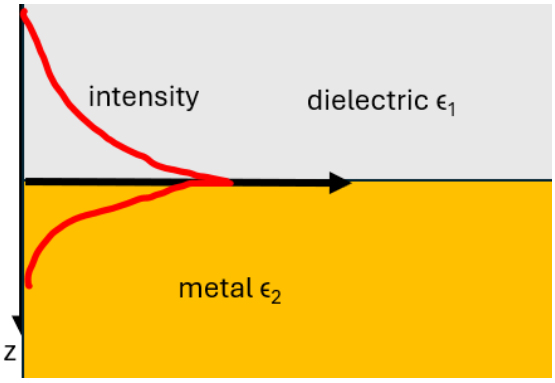


**Figure 4**. Evanescent field that decays exponentially into the two half spaces.

Altogether, one obtains a system that is composed of an electromagnetic wave in the dielectric medium and an oscillating electron plasma in the metal, where both modes have an exponentially decaying evanescent character (see Fig. 5 and Ref. 7, 9).

Let us now derive the dispersion relations for surface plasmons. For the wave vector we get:

$$|\mathbf{k}_{1(2)}|^2 = \epsilon_{1(2)} k_0^2 = \beta^2 + k_{1(2),z}^2 = \beta^2 - \kappa_{1(2)}^2$$

here, $k_0 = \omega/c$ is the vacuum wave vector of light with frequency ω. Hence our previous relation

$$\frac{k_{1,z}}{\epsilon_1} = \frac{k_{2,z}}{\epsilon_2}$$

takes the form

$$\beta = \frac{\omega}{c}\sqrt{\frac{\epsilon_1 \epsilon_2}{\epsilon_1 + \epsilon_2}} \qquad (1)$$

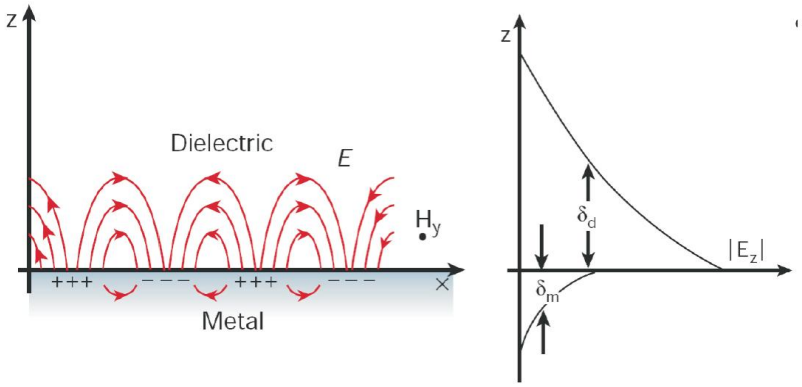


**Figure 5**. Schematics to summarize the nature of SPPs [7]. They are a coherent oscillation of electrons at the interface between a metal and a dielectric material. SPPs are transverse magnetic in character (H is in the y-direction), and the generation of surface charge requires an electric field

normal to the surface (left). The combined character also leads to the field component perpendicular to the surface being enhanced near the surface and decaying exponentially with distance away from it. The field in this perpendicular direction is said to be evanescent, reflecting the bound, non-radiative nature of SPPs, and prevents power from propagating away from the surface. In the dielectric medium above the metal, typically air or glass, the decay length of the field, $\delta d$, is of the order of half the wavelength of light involved, whereas the decay length into the metal, $\delta m$, is determined by the skin depth (right).

Together with the information of the frequency dependence of $\varepsilon_{1(2)}(\omega)$, one can derive for the dispersion relation $\omega(k_{SPP})$. Under the assumption that $\varepsilon_1(\omega)$ in the dielectric is approximately constant and using the Drude approximation for $\varepsilon_2$, one obtains a dispersion relation as shown in Fig. 6.

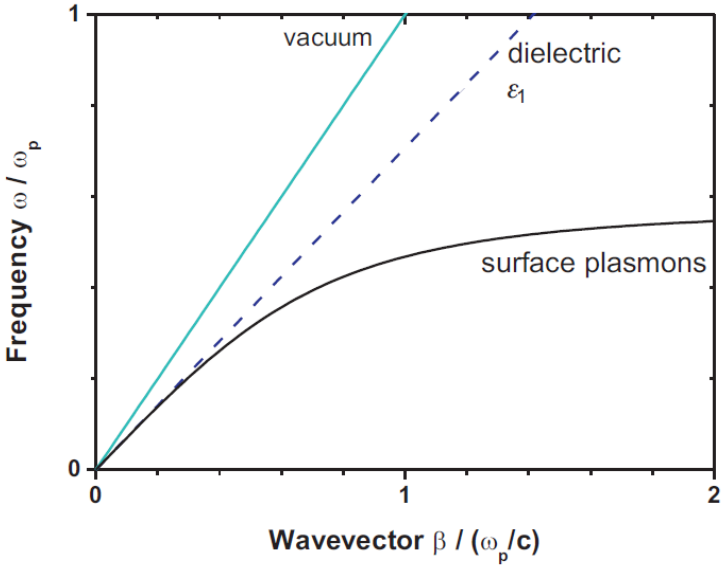


**Figure 6**. Dispersion relation of surface plasmons compared to light in vacuum and in the dielectric medium [9].

One realizes that the SPP dispersion relation completely resides below the light cones and thus SPPs cannot be excited by direct illumination, as energy and momentum conservation ($\omega_{light} = \omega_{SPP}$ and $k_{light} = k_{SPP}$) cannot be fulfilled at the same time. Instead, in order to excite SPPs, a momentum transfer has to be established. Techniques to achieve this will be discussed in the following.

## 2. **Experimental background**

### 2.1 **Coupling light to surface plasmon polaritons and sensing**

To couple light to the SPP mode, energy and momentum conservation must be maintained. Therefore, the incoming beam has to match its momentum to that of the SPP. In the case of p-polarized light (polarization occurs parallel to the plane of incidence), there are three main techniques by which the missing momentum can be provided. The first makes use of prism coupling to enhance the momentum of the incident light. The second involves scattering from a topological defect on the surface, such as a subwavelength features or hole, which provides a

convenient way to generate SPPs locally. The third makes use of a periodic structure in the metal's surface. S-polarized light (polarization occurs perpendicular to the plane of incidence) cannot excite SPPs.

Otto and Kretschmann configurations are the two well-known simple methods to achieve coupling using a prism. In the Otto setup [2], light illuminates the wall of a prism and it undergoes total internal reflection. An air gap (or a spacer of low index) less than a few optical wavelengths thick) provides the tunnel barrier across which radiation couples, via the evanescent component of the totally reflected wave, to SPPs at the air (dielectric) metal interface (e.g. gold), as shown in Fig. 7(a). By varying the angle of incidence of p-polarized radiation at the prism/dielectric interface, one can vary the momentum in the *x*-direction and this allows for simple tuning through the coupling condition, called surface plasmon polariton resonance (SPR). The other alternative and simpler geometry was realized by Kretschmann [3]. Rather than using a dielectric spacer the metal itself could be used as the evanescence tunnel barrier provided it is thin enough to allow radiation to penetrate to the other side. All that is now needed is a prism with a thin coating of some suitable metal, as shown in Fig. 7(b).

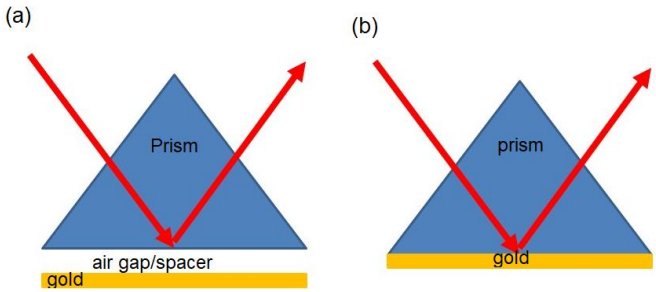


**Figure 7**. (a) Otto configuration. (b) Kretschmann configuration.

The sensing activity can be performed once efficient coupling is obtained. A schematic of a SPR-based sensor is depicted in Fig. 8. A glass prism is coated with a thin layer of a noble metal (or brought near to using Otto configuration) to create a biosensor surface. Antibody or another type of biomolecules (chemicals) immobilized on the sensor surface is also shown. At a particular angle ($\theta_o$) the incoming wave couples to SPP. This special incidence angle is called SPR angle. At the SPR angle reflectivity hence drops to a minimum as shown in the figure (right). However, the binding of biomolecules onto the sensor's surface affects the SPR condition: the refractive index of the dielectric component increases and shifts the SPR angle to another value ($\theta_1$). The measurement of the SPR-angle shift offers an opportunity to measure molecular binding to the sensor's surface or other physical quantities (e.g. index of refraction) [8].

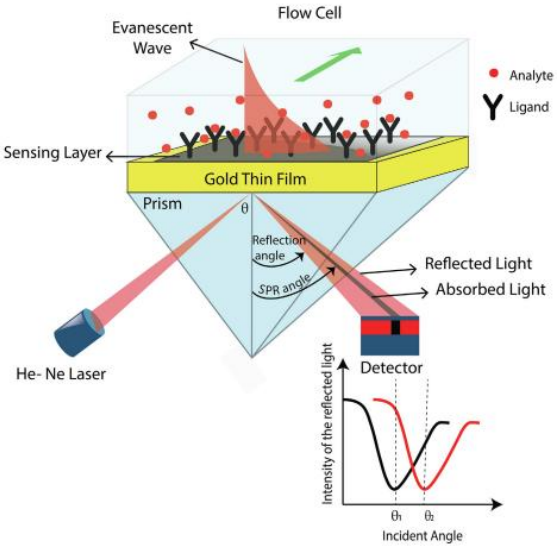


**Figure 8**. Schematics of a SPR-based sensor [8]. The SPR-angle shift provides information about the efficiency of binding to the sensor's surface or directly measure the physical quantities under investigation.

### 2.2 Experimental setup for detecting SPR

The optical setup to measure the SPR of thin gold films (50 nm-thick) is depicted in Fig. 9, similar to the configuration discussed in Ref. [10] and it has the following elements:


**Figure 9**. Optical setup for directly measuring the plasmon extinction.

*Light source*: A He–Ne laser (λ = 632.8 nm) with 2 mW output power. The polarization of the laser can be manipulated by using a linear polarizer and a half-wave plate.

*Prism and gold thin film*: A high-index prism (index of refraction $n_p$ = 1.62) is used to couple light to the SPP mode. Instead of depositing a thin film of gold on the prism, glass slides are already prepared and adapted on one side of the prism with an index matching liquid (index of refraction $n_L$ = 1.52).

*Manual rotation stage and light path*: A manual rotation stage with an accuracy of 1° is used to measure the angle $\theta_{ext}$ as shown in Fig. 10. The prism is positioned on the stage so that the 180°

angle corresponds to the laser beam being back reflected to the laser. This allows us to directly measure the angle marked $\theta_{ext}$.

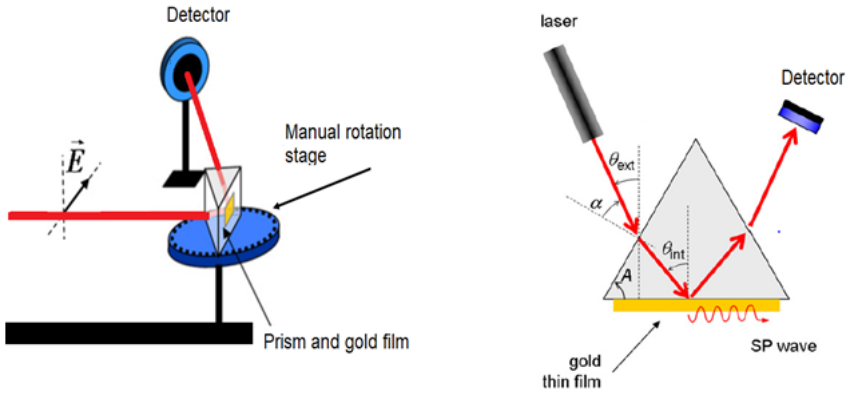


**Figure 10**. Monochromatic p-polarized light impinges on a prism in a total reflection configuration. A gold film of thickness around 50 nm is placed on the prism so that it collects the evanescent waves produced by total internal reflection and the SPP wave is launched at the gold/air interface if the angle is set at the right values. The light intensity reflected by the prism is measured with a photodiode, which shows a minimum when the coupling with the SPP wave occurs [modified version of Ref. 10].

The value of $\theta_{int}$ is obtained by the following relation, where the angles are oriented according to the counter-clockwise orientation of the plane, as indicated in Fig. 10 (right).

$$\theta_{\text{int}} = \arcsin \frac{\sin(\theta_{\text{ext}} - A)}{n} + A. \qquad (2)$$

According to the discussion in the previous session (see equation 1), the condition for coupling the excitation wave with the SP wave now takes the form:

$$(n \sin \theta_{\text{int}})^2 = \frac{\varepsilon_1(\omega) \cdot \varepsilon_2(\omega)}{\varepsilon_1(\omega) + \varepsilon_2(\omega)}. \qquad (3)$$

Note that in the case of gold/air interface, $\epsilon_2 = 1$, but in more general cases medium 2 is a dielectric medium such as a liquid or molecules adsorbed on the gold surface.

Remember that in the experiment one measures the external angle $\theta_{ext}$ and using equation (2) the internal angle $\theta_{int}$ is determined. Equation (3) helps to relate the internal angle with the dielectric constants.

*Detection*: The reflected beam is collected with a photodiode and the photodiode is chosen so that the sensor area is greater than the cross-section of the laser beam. The detector is moved manually for each value of the incidence angle.

## 3. Procedures

### 3.1 Excitation of SPP

*Step 1*. Check the setup and the necessary equipment required for the experiment, measure the power of the laser and check the polarization orientation.

*Step 2*. Verify that s-polarized incident radiation does not excite SPPs.

*Step* 3. Find the SPR angle for p-polarized light as shown in Fig. 11. Repeat the measurement for 10 times only near the transmission dip, in order to be able to apply statistics for the error analysis.

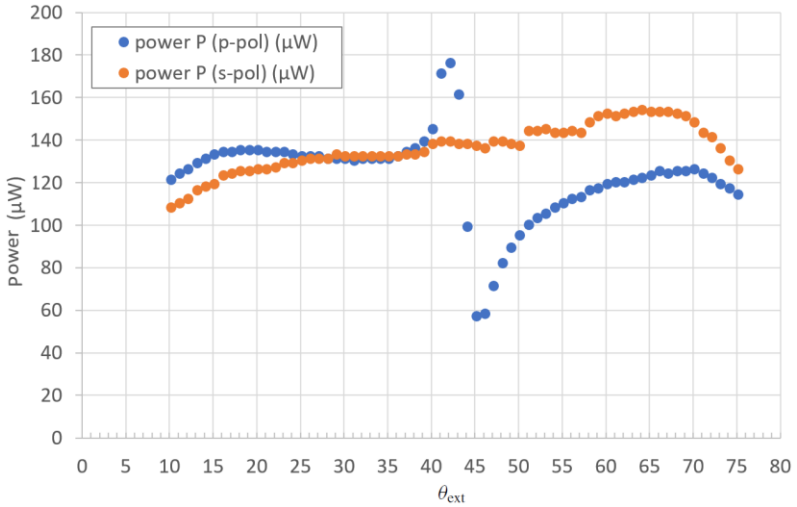


**Figure 11**. Excitation of SPPs using p-polarized incident light.

### 3.2 Sensing of fluid

*Step 1*. Put droplet of water on the measured gold film. Carefully follow the procedures as described by your supervisor.

*Step 2*. Measure the shift in the SPR angle due to the water layer. Repeat the measurement 10 times around the transmission dip. Use this information to determine the index of refraction of water. Discuss the source of errors, analyze the data accordingly (e.g., standard deviation, error propagation) to estimate the experimental error on the measured refractive index. Compare the theoretical value of the index of refraction of water ($n_w$ = 1.33) with the measured one.

### 3.3 **Data analysis and report format**

The excitation of surface plasmon polaritons results into a reflectance dip. The shape of the dip can be complex, based on the actual configuration of the prism, thin films and coupling conditions.

A suitable physical model to fit the resulting curve is the so-called Fano line shape [11]. Originally introduced to explain asymmetries in atomic excitation spectra, it has become popular in photonics [12].
The fitting function consists of three parameters: the coupling angle ($\theta_0$), the linewidth $\gamma$ and the Fano parameter $q$, which is responsible for the asymmetry. The function is expressed as follows:

$$R(\theta, \gamma, q) = A \frac{[q.\gamma/2 + (\theta - \theta_0)]^2}{(\gamma/2)^2 + (\theta - \theta_0)^2} + B.$$

where $R$ is the power of the reflected light, $A$ and $B$ are the amplitude and background offset, respectively. Changing the Fano asymmetric parameter $q$ allows to fit the data better. $q = 0$ corresponds to symmetric Lorentzian function. Figure 12 shows the plot for $q = 0$ and $q = 1.0$.

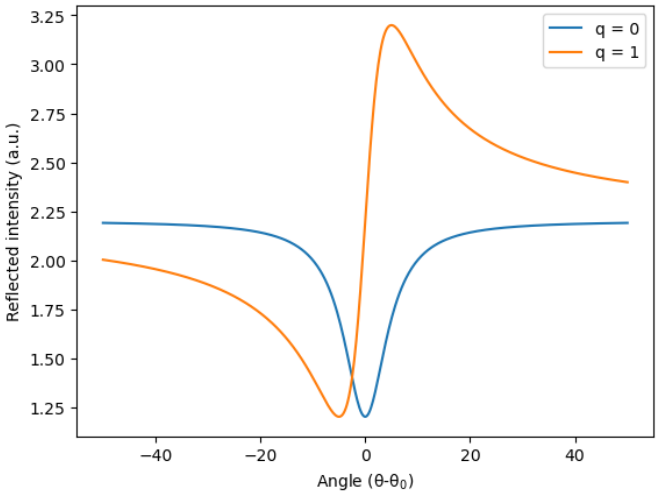


Figure 12. Plot of the reflected light intensity versus the coupling angle for two values of the parameter $q$ demonstrating the asymmetric Fano line-shape.

Remind that a good lab report does more than presenting data; it demonstrates the writer's comprehension of the concepts behind the data. Merely recording the expected and observed results is not sufficient; you should also identify how and why differences occurred, explain how they affected your experiment, and show your understanding of the principles the experiment was designed to examine.

Bear in mind that a format, however helpful, cannot replace clear thinking and organized writing. You still need to organize your ideas carefully and express them coherently. Typical components to be fulfilled are: Title Page, Abstract, Introduction, Methods and Materials (or Equipment), Experimental Procedure, Results, Discussion, Conclusion, References.

## 4. References


1. G. Mie, Beiträge zur Optik trüber Medien, speziell kolloidaler Metallösungen, Ann. Phys., 25, 377 (1908).
2. A. Otto, Excitation of nonradiative surface plasma waves in silver by the method of frustrated total reflection, Z. Phys. 216, 398 (1968).
3. E. Kretschmann, Die Bestimmung optischer Konstanten von Metallen durch Anregung von Oberflächenplasmaschwingungen, Z. Phys. 241, 313 (1971).
4. B. Hecht, H. Bielefeldt, L. Novotny, Y. Inouye, and D.W. Pohl, Local excitation, scattering, and interference of surface plasmons, Phys. Rev. Lett. 77, 1889 (1996).
5. J. Pendry, Playing tricks with light, Science 285,1687 (1999).
6. S.A. Maier, Plasmonics: Fundamentals and Applications (Springer Science and Business Media, 2007).
7. W.L. Barnes, A. Dereux, and T.W. Ebbesen, Surface plasmon subwavelength optics, Nature 424, 824-830 (2003).
8. F. B. K. Eddin, Femtomolar detection of dopamine using surface plasmon resonance sensor based on chitosan/graphene quantum dots thin film. Spectrochimica Acta Part A: Molecular and Biomolecular Spectroscopy, 263, 120202 (2021).
9. Humboldt-Universität zu Berlin. (n.d.). Plasmonics. Retrieved April 14, 2025, from https://www.physik.hu-berlin.de/de/nano/lehre/Gastvorlesung%20Wien/plasmonics/@@download/file/Plasmonics.pdf
10. O.Pluchery, R.Vayron, and K. Van, Laboratory experiments for exploring the surface plasmon resonance, Eur. J. Phys. 32, 585 (2011).
11. U. Fano, Effect of configuration interaction on intensities and phase shifts, Phys. Rev. **124**, 1866 (1961)
12. M. F. Limonov, M. V. Rybin, A. N. Poddubny, Y. S. Kivshar, Fano resonance in photonics, Nature Photonics, **11**, 543 (2017).